

1
2
3
4
5
6
7
8
9
10
11
12
13
14
15
16
17
18
19
20
21
22
23
24
25
26

Exploring the cytotoxic mechanisms of Pediocin PA-1 towards HeLa and HT29 cells by
comparison to known bacteriocins.

George P. Buss^{1*}, Cornelia Wilson¹

¹ Canterbury Christ Church University, N Holmes Road, Canterbury CT1 1QU

*Corresponding author

27 Abstract

28 The purpose of this study was to explore potential mechanisms of cytotoxicity towards HeLa and
29 HT29 cells displayed by Pediocin PA-1. We did this by carrying out sequence alignments and 3D
30 modelling of related bacteriocins which have been studied in greater detail: Microcin E492,
31 Enterocin AB heterodimer and Divercin V41. Microcin E492 interacts with Toll-Like Receptor 4 in
32 order to activate an apoptosis reaction, sequence alignment showed a high homology between
33 Pediocin PA-1 and Microcin E492 and 3D modelling showed Pediocin PA-1 interacting with TLR-4 in a
34 way reminiscent of Microcin E492. Furthermore, Pediocin PA-1 had the highest homology with the
35 Enterocin heterodimer, particularly chain A; Enterocin has also shown to cause an apoptotic
36 response in cancer cells. Based on this we are led to strongly believe Pediocin PA-1 interacts with
37 TLRs in order to cause cell death. If this is the case it would explain the difference in cytotoxicity
38 towards HeLa over HT29 cells, due to difference in expression of particular TLRs. Overall, we believe
39 Pediocin PA-1 exhibits a dual effect which is dose dependant, like that of Microcin. Unfortunately,
40 the COVID-19 pandemic meant that we were unable to carry out experiments in the lab, and the
41 unavailability of important data meant we were unable to make solid conclusions but rather
42 suggestions. However despite this we have still been able to highlight interesting findings and how
43 these could be translated into future research and therapeutics in order to improve the quality of
44 treatment and life of cancer patients.

45

46

47

48

49

50

51

52

53 Introduction

54 From 2015-2017 there were around 367,000 people given a new diagnosis of cancer every year, with
55 breast, prostate, lung and bowel cancer accounting for 53% of these new diagnosis¹. This study
56 looks at the effect of Pediocin PA-1 on HT-29 cells, a cell line isolated in 1964 from colonic
57 adenocarcinoma cells²; and HeLa cells, a cell line isolated in 1951 from cervical cancer cells³.
58 Considering the neurotoxic effects of conventional therapies, such as chemotherapy and
59 radiotherapy - from minor cognitive effects to major pathology such as encephalopathy^{4,5}, the
60 exploration of bacteriocins as a novel anti-cancer therapy allows the opportunity for a better quality
61 of life for cancer patients undergoing treatment. Further still, targeted therapies have shown to
62 improve the longevity and quality of patients lives^{6,7}. Bacteriocins offer the opportunity for the
63 development of highly targeted therapies whilst still ensuring an even greater quality of life.

64 Pediocin PA1 is a 62-amino acid long class IIa bacteriocin expressed in *Pediococcus acidilactiti* (gram-
65 positive bacteria) generally in response to stress and/or ultraviolet light^{8,9}. Bacteriocins are catatonic
66 peptides produced by all types of bacteria that are non- immunogenic, biodegradable and can
67 colonise cancer cells with specific toxicity¹⁰. Pediocin has been shown to display cytotoxic effects
68 towards HeLa and HT29 cells, with a greater cytotoxic effect towards HeLa over HT29¹¹. Whilst there
69 have been several studies looking into the cytotoxic effect of Pediocin, the mechanism has never
70 been studied in as great detail as other bacteriocins. This is a comparative study against other
71 bacteriocins which have been researched in greater detail; it is hoped that by carrying out sequence
72 alignments and 3D modelling we will be able to identify potential mechanisms of actions by Pediocin
73 PA-1. Microcin E492 and Enterocin AB heterodimer have both been shown to induce apoptosis,
74 indicating a protein interaction^{12,13,14}. Therefore by comparing sequence alignment and analysing 3D
75 models we hope to identify similarities within the structure of Pediocin A1 compared to these
76 bacteriocins which may give further insight into it's mechanism of action.

77 Furthermore, Divercin V41 is also a class IIa bacteriocin which was shown to have no cytotoxic effect

78 against HT29 – being of the same class of toxin as Pediocin PA-1 we hope to identify what is different
79 between these two bacteriocins, and as such gain greater insight into Pediocin PA-1’s mechanism of
80 action.

81

82 There has been some controversy when it has come to the mechanism of Pediocin PA-1: four
83 cysteine residues within the structure have been shown to form a disulphide bridge which forms a
84 poration complex in target membrane, leading to cell death¹⁵. It has also been found
85 that Pediocin PA-1 is able to function in the absence of protein receptors¹⁶. However,
86 Enterocin has also been shown to cause permeabilization of the lipid bi-layer whilst also inducing
87 apoptosis by bio-energetic collapse¹⁷ – this is indicative of protein interaction with
88 Toll-Like Receptors (TLRs) to trigger a caspase response. Other bacteriocins have also been shown
89 to have this dual mechanism of cytotoxicity – which we discuss later in this paper. Therefore, we
90 argue that it is likely Pediocin PA-1 also has a dual mechanism of cytotoxicity towards cancer
91 cells.

92

93 Bacteriocins offer a potential advancement in the treatment of cancer, as most target cancer cells
94 whilst having very limited interaction with human cells. This is due to the negative charge of cancer
95 cells¹⁸, the negative charge has been labelled the “Warburg Effect” which explains the
96 secretion of more than thirty times the amount of lactic acid than healthy cells, by cancer cells^{19,20}.

97 Bacteriocins have an overall positive charge, and thus target cancer cells over human cells¹⁰.

98 Pediocin PA-1 itself is nontoxic, nonimmunogenic being used as a bio-food preservative
99 protecting against *Listeria monocytogenes*²¹, other bacteriocins are also widely used in
100 the same manner. In this way we know that Pediocin is safe for human consumption.

101

102 Whilst this study had it’s limitations due to the COVID-19 pandemic preventing us from carrying out
103 *in vitro* experiments in the lab, we were still able to utilise bioinformatic tools to gain a further

104 insight into the potential mechanisms of Pediocin PA-1. Whilst also commenting on other
105 bacteriocins. In this way we were able to give a strong argument for further study, as well
106 as highlighting the potential use of bacteriocins as novel cancer therapeutics.

107

108

109

110

111

112

113

114

115

116

117

118

119

120

121

122

123

124

125

126

127

128

129 Methodology

130 Accessing Protein Sequences

131 UniProt was used to access the protein sequences in this analysis (see figure 1)]. UniProt is an
132 opensource database maintained by the UniProt consortium. The database is an amalgamation of
133 Swiss-Prot, TrEMBL and the PIR Protein Sequence Database. It contains protein sequence and
134 functional information often derived from primary genome research and analysis.
135 Pediocin PA1 and the other bacteriocins were located on the UniProt database, the PBD 3D structure
136 was then downloaded. In the case of Divercin V41 there was no current PBD model, so the protein
137 sequence was downloaded and modelled using Swiss Model^{23,24,25}.

138 Sequence Alignment

139 Protein sequences were downloaded from UniProt and then aligned using MultiAlin^{22,26}. Pediocin,
140 Divercin, Microcin and Enterocin were uploaded to the server, default parameters of 90% high
141 consensus and 50% low consensus were used. The sequence alignment was exported as a table
142 image.

143 Model Analysis

144 Once downloaded, PDB files were viewed in VMD²⁷. VMD is an opensource modelling software
145 which allows visualisation and analysis of protein structures. VMD can also be used to simulate and
146 analyse the molecular dynamics of a system. We were able to use VMD to identify interacting
147 residues that appeared significant to each protein structure and propose a mechanism of action
148 based on this and previous *in-vitro* findings. It is worth noting that in the case of TLR-4 we located an
149 accurate model of the LPS Ra complex of E. coli and TLR-4 interacting from RCSB PDB (named 3FXI).
150 We then isolated the TLR-4 using the viewing tool of RCSB PDB and downloaded the .pdb file²⁸.

151

152 Swiss-model

153 Divercin V41 did not have a published PBD file on UniProt and we were unable to identify any
154 previous research which had attempted to deduce the 3D structure. Therefore, we used Swiss-
155 Model to derive a predicted structure for Divercin V41, this was downloaded as a PBD file and
156 viewed in VMD. We were also unable to locate a fully devised 3D structure for Enterocin B, so Swiss-
157 model was also used in this instance. SWISS-MODEL is an automated protein structure homology-
158 modelling server^{23, 24, 25, 29}.

159

Protein	Acession_Number
Pediocin PA1	P29430
Divercin V41	Q9Z4J1
Microcin E492	A0A652PYJ5
Enterocin A	AF240561
Enterocin B	AYG20277

160
161
162
163

Fig 1. Table showing the proteins analysed and their corresponding accession numbers as according to UniProt²².

164
165
166
167
168
169
170
171
172

173 Results Microcin E492

174 Microcin E492 is a highly hydrophobic 7.9kDa bacteriocin produced by *Klebsiella pneumoniae*^{30, 31}.

175 When co-cultured with HeLa cells cytotoxic effects observed were typical of apoptosis, these
176 included: cell shrinkage, DNA fragmentation, caspase-3 activation and loss of mitochondrial
177 membrane potential; cell necrosis was also observed at higher doses of Microcin¹³. Additionally the
178 presence of zZAD-fmk (caspase inhibitor) completely blocked the cytotoxic effect of Microcin¹³.

179 Caspase 3- activation is associated with the activation of toll-like receptor 4, therefore during the 3D
180 modelling analysis we included toll-like receptor 4 (TLR-4) to observe how Microcin E492 interacts
181 with it³².

182 Sequence Alignment

183 A sequence alignment was performed between Microcin E492 and Pediocin PA-1. Microcin E492 is a
184 significantly larger protein than Pediocin, however despite this difference there is significant
185 homology between the two proteins (See figure 2). Largely, the homology is of low consensus with
186 only fourteen residues aligning with a high consensus.

Fig 2. Sequence comparison of Microcin E492 and Pediocin A1 (Pediocin). Low consensus alignments (50%) are represented as blue letters, whilst high consensus alignments (90%) are represented as red letters. Microcin is significantly larger than Pediocin A1, whilst there is homology this a mainly low consensus homology with fourteen residues of high consensus²⁶.

187

188 3D Modelling: VMD

189 Unfortunately, despite extensive research there was no 3D model available for Microcin E492,
190 therefore we used SWISS-MODEL to build a 3D model based on the fasta sequence obtained from
191 RCSB PDB³³. This was then downloaded as a .pdb file and viewed in VMD alongside the toll-like
192 receptor-4. The model built using SWISS-MODEL had a sequence identity of 30%, whilst this is not
193 ideal it is, to the best of our knowledge, the best model of Microcin E492 available at the time of
194 research.

195 TLR-4 is arranged as a heterodimer of two chains: A and B, they are arranged in a helical structure
196 and the ends of each chain come fold around each other. According to VMD analysis (see figure 3),
197 Microcin E492 sits in the middle of the heterodimer where both chains meet, interacting with both
198 chains. Common contact residues for both chain A and B with Microcin included mainly hydrophobic
199 residues: glycine, valine, phenylalanine, leucine and, isoleucine.

200 In order to explore the possibility that Pediocin PA-1 also could interact with TLR-4 we carried out 3D
201 modelling of Pediocin PA-1 interacting with TLR-4 too (see figure 4). Whilst being smaller than
202 Microcin E491, Pediocin also sat in between the receptor interacting with both chains as they met.
203 Common contact residues were the same as Microcin E492: glycine, valine, phenylalanine, leucine
204 and isoleucine.

205 **Fig 3.** 3D model of Microcin (A) and Microcin interacting with TLR-4 (B) produced using
206 the .pdb file imported from RCSB PDB to VMD. TLR-4 has been drawn in lines in order to
207 distinguish between Microcin and TLR-4 A) Microcin appears mainly globular in shape
and has small yet frequent regions of polarity. B) TLR-4 is arranged as a heterodimer of
two chains converging in the centre, Microcin interacts with both chains in the middle of
this convergence²⁷.

208 **Fig 4.** 3D model of Pediocin A1 interacting with TLR-4 produced using the .pdb file
imported from RCSB PDB to VMD. TLR-4 has been drawn in lines in order to distinguish
209 between Pediocin A1 and TLR-4. Like Microcin, Pediocin appears mainly globular in
210 shape, the TLR-4 is arranged as a heterodimer of two chains converging in the centre,
211 Pediocin A1 interacts with both chains in the middle of this convergence²⁷.

208

209

210

211

212

213

214 Results: Enterocin

215 Enterocin is a class IIa bacteriocin, it is a heterodimer formed from chains A and B and is produced by
216 *Enterococcus faecium*. It is used within different food products due to its anti-listerial properties¹⁴,
217 ¹⁷. The heterodimer is formed by strong hydrophobic forces of leucine, isoleucine, tyrosine, glycine
218 and phenylalanine residues³⁴. Enterocin also displays cytotoxic effects towards HT29 and HeLa cells,
219 as a heterodimer these effects were greater. Enterocin also displayed a greater effect towards HeLa
220 than HT29 cells¹⁴.

221 Sequence alignment and 3D models of Enterocin A and B were completed in order to distinguish
222 whether there were any shared features between the mechanism of action of Pediocin and the
223 Enterocin heterodimer.

224

225 Sequence Alignment

226 A sequence alignment was carried out for PediocinA1, Enterocin A and, Enterocin B. The previous
227 research has highlighted that Enterocin A and B potentially have different mechanisms of action,
228 therefore by comparing Pediocin PA-1 to each homodimer it can give further insight into the exact
229 mechanism of action of Pediocin PA-1. The highest homology is seen between Pediocin and
230 Enterocin chain A, however there is still a significant homology between Pediocin and Enterocin B
231 (see figure 5). This could indicate that Pediocin has a dual mechanism of action incorporating how
232 Enterocin functions as a heterodimer.

Fig 5. Sequence comparison of Enterocin A (EntA), Enterocin B (EntB) and Pediocin A1 (Pediocin). Low consensus alignments (50%) are represented as blue letters, whilst high consensus alignments (90%) are represented as red letters. Pediocin has a high level of alignment with both Enterocin A and Enterocin B²⁶.

233

234

235

236 3D Modelling Analysis

237 Enterocin A is significantly smaller than Enterocin B, 712 residues compared to 2125 residues.

238 Enterocin B also appears to have a greater charged surface than Enterocin B. It is also interesting to

239 note that both molecules have two cysteine residues (shown in yellow) on their surface (see figure

240 7), however when acting as a homodimer these residues do not seem to be involved and there were

241 no disulphide bridges detected on analysis. Further analysis revealed a hydrophobic surface of

242 Enterocin, with exposed residues including: Val'15, Trp'33, Lys'43, Tyr'2, Trp'33 and Ala'32. This is in

243 keeping with the previous findings¹⁴.

244 **Fig 6.** 3D model of Enterocin A produced using the .pdb file imported from
245 RCSB PDB to VMD. A) shows the positive x/y axis angle of Enterocin A,
246 whilst B) shows the negative x/y angle. Analysis reveals regions of polar
and charged residues (shown in red) of the surface of Enterocin B, as well
as two cysteine residues (shown in yellow) on the surface of Enterocin A²⁷.

247 **Fig 7.** Devised 3D Model of Enterocin B alongside the Global Quality Estimate (C).
248 Analysis reveals areas of polarity (A) and one cysteine residue (B). The overall sequence
249 identity was 7.69% however, there is currently no 3D model of Enterocin B on it's own,
therefore this is the most accurate representation to date^{23, 24, 25}.

250

251

252

253

254

255

256

257 Divercin V41

258 Divercin has previously been shown to have a similar homology to Pediocin whilst showing no anti-
259 tumour properties towards HT29 cells³⁶. Therefore we performed sequence alignment and 3D
260 modelling of Divercin V41 in order to try and understand why, despite the similar homology, one
261 shows anti-tumour effects towards HT29 cells and not the other.

262 The sequence comparison of Divercin V41 and Pediocin PA-1 shows a high homology, with high
263 consensus (90% consensus) proteins including hydrophobic residues glycine and isoleucine;
264 amphipathic residues tyrosine and tryptophan; and charged residues of glutamic acid (see figure 8).
265 Charged residues of glutamic acid are often used in the formation of salt bridges. Low consensus
266 proteins (50% consensus) include: hydrophobic residues glycine, isoleucine, alanine; charged
267 residues lysine, aspartic acid, and lysine; polar charged residues histidine and glutamine. Polar
268 charged residues are often associated with hydrogen bond formation through acting as protein
269 donators and acceptors.

270 **Fig 8.** Sequence comparison of Divercin V41 and Pediocin A1 (shown as
271 PPA1_PEDAC). Low consensus alignments (50%) are represented as blue
letters, whilst high consensus alignments (90%) are represented as red
letters. The overall consensus sequence is low alignment²⁶.

272 The devised 3D model from SWISS MODEL (see figure 9) predicted Divercin V41 to be more linear in
273 shape compared to Pediocin PA-1, which is more globular. Pediocin PA-1 is also shown to have a
274 greater surface polarity than Divercin V41. Depending on the mechanism of action, both the
275 difference in shape and polarity could go some way to explain why Divercin V41 does not show anti-
276 tumour effects on HT29 cells despite the relatively high homology with Pediocin PA-1.

277 **Fig 9.** Devised 3D Models of Divercin V41 (B) and Pediocin A1 (A) alongside their Global
Quality Estimate respectively (C and D). Pediocin is shown to have a greater surface
polarity than Divercin. There is only a 37.50% sequence identity for the Divercin V41
model compared to the Pediocin A1 model, however due to the lack of data this is the
most accurate model that we are aware of^{23, 24, 25}.

278 VMD analysis revealed exposed residues included charged residues: Asp'41, Lys'25, Lys'36 and
279 Lys'65; polar residues: Asn'29, Asn'34, Gln'44, Gln'51, Tyr'2 and Tyr'32; hydrophobic residues: Gly'5,
280 Gly'39 and Gly'64; as well as amphipathic Trp'42. There were also three Cysteine residues on the -y
281 axis of the Divercin V41. Despite this, there were no salt bridges detected on analysis.

282

283

284

285

286

287

288

289

290

291

292

293

294

295

296

297

298

299 Discussion

300 Like Pediocin PA-1, Microcin E492 has shown cytotoxic effects against HeLa cells. The observations of
301 this cytotoxicity are inductive of apoptosis both biochemically and morphologically¹³. Further
302 analysis revealed this apoptosis was due to caspase 1 and 3 activation. Definitive support can be
303 found in the same study, as the use of zZad-fmk (a general caspase inhibitor) inhibited the cytotoxic
304 effect of Microcin. Caspase 3 activation has been linked to the activation of TLR-4³⁶, therefore we are
305 confident in our conclusion that Microcin must bind to TLR-4. Caspase 1 activation has been linked
306 to the efflux of potassium ions, which activates the NLRC4 (nucleotide-binding oligomerization
307 domain and leucine-rich repeat containing receptors) inflammasome pathway leading to the
308 assembly of caspase 1³⁷. Considering that when high doses of Microcin E492 were administered to
309 HeLa cells necrosis was observed¹³, alongside the previously mentioned caspase-1 activation, and
310 the link between programmed necrosis and membrane pore formation³⁸. With this in mind, it is clear
311 that microcin has a dual mechanism of apoptosis and pore-formation.

312 Whilst Pediocin PA-1 is much smaller in size compared to Microcin E492, they are both globular in
313 shape as well as having residues of similar properties. Furthermore, the 3D modelling analysis
314 revealed that they also bind to TLR4 in the same manner. Pediocin PA-1 was shown to have a
315 greater cytotoxic effect against HeLa cells compared to HT29 cells – however the researchers were
316 only able to speculate¹¹, if Pediocin PA-1 does interact with TLR-4 then one potential reason for this
317 difference could be because TLR-4 is over-expressed in HeLa cells³⁹. On the other hand, although
318 TLR-4 is expressed in human colon cells, this appears to be mainly limited to crypt cells – alongside
319 TLR-2⁴⁰; therefore, we would not expect as high levels of TLR-4 to be expressed in HT29 cells. This
320 goes some way to explaining why we do not observe as extreme an effect in HT29 cells as we do in
321 HeLa.

322 We did consider the possibility of Pediocin PA-1 acting on other receptors, however due to the
323 limitations of experimental data available, and the COVID-19 restrictions which prevented us from

324 carrying out lab work we were unable to effectively look at this. It would be interesting to explore
325 the effect Pediocin PA-1 may have on TLR-2 – which has been shown to have a major role in TLR2
326 recognition⁴¹.

327 Divercin V41, like Pediocin PA-1, is produced from gram-positive bacteria; microcin however, is
328 produced from gram-negative bacteria. Therefore, it would be interesting to explore how TLR-2
329 expression effects cytotoxicity, especially considering its important role in the recognition of gram-
330 positive bacterial components. If Pediocin PA-1 does in fact interact with TLR-2, then this could go
331 some way to explaining why Divercin, despite the high homology to Pediocin PA-1, does not display
332 a cytotoxic effect to HT29 cells. Unfortunately, Divercin V41 has not been tested alongside HeLa
333 (with high TLR-2/4 expression) and therefore it is difficult to compose more than a speculative
334 argument in regard to the mechanism. However, this observed difference in cytotoxicity despite high
335 homology does give strong indication that Pediocin PA-1, like Microcin, has several cytotoxic effects
336 which may be dose dependant. Going forward it would be interesting to carry out a comparative
337 study on the cytotoxicity of Pediocin PA-1 and Divercin V41 in HeLa and HT29 cells of wild type, TLR-
338 2 knockout and TLR-4 knockout.

339 The Enterocin AB heterodimer has also been shown to be an apoptotic inducer of HeLa and HT29,
340 which means it must also interact with a TLR, interestingly both homodimers of Enterocin induce an
341 apoptosis however this effect is enhanced when acting as a heterodimer¹⁴. The study did not use
342 caspase inhibitors or identify the caspase that induced apoptosis, therefore it is not possible to
343 comment on what TLR Enterocin AB acts on, or whether they act on separate TLRs each – hence the
344 enhanced effect when working as a heterodimer. Pediocin PA-1 and Enterocin A have the highest
345 homology of all the compounds assessed and are the most similar in shape and structure. It is
346 interesting then that inhibition of HeLa growth increased from 38.42% inhibition, when Enterocin B
347 only was being used, to 78.83% growth inhibition when Enterocin A was added¹⁴. Both Pediocin PA-1
348 and Enterocin A have cysteine residues, we know that in Pediocin PA-1 cystine residues lead to the

349 formation of two disulphide bonds which stabilise the hairpin conformation of the two beta sheets.
350 Therefore, we believe it is from studying Enterocin A which will give us the best clues about the
351 mechanism of action of Pediocin PA-1. A possible experiment could be to use TLR knockout HeLa
352 cells alongside Enterocin A to observe the effect of inhibition, fluorescent microscopy could also be
353 used to visualise the toxin with the cell.

354 As well as evidence that Pediocin PA-1 induces apoptosis, it has been shown to target lipid vesicles
355 as a dose dependant efflux of carboxyfluorescein (CF). Imaging showed results were light scattering,
356 meaning the lipid membrane was permeabilised but the overall structure was not changed¹⁵. Further
357 support for this mechanism was seen when Pediocin PA-1 remained functional in the absence of
358 protein receptors⁴², from this it was concluded that Pediocin did not interact with proteins, but
359 rather was pore forming. We would argue that instead of this being Pediocin's only mechanism of
360 cytotoxicity, it is one of at least two. The toxins in this research are all class II bacteriocins, class II
361 bacteriocins have all been recognised for their pore-forming mechanisms in bacteria⁴³. However, as
362 highlighted above many have been shown to cause bioenergetic collapse secondary to apoptosis,
363 Microcin as an example was shown to cause apoptosis however at high doses, necrosis was
364 observed. This clearly shows class IIa bacteriocins appear to have a dose dependant cytotoxic effect.

365 We strongly feel that the findings of this study provide a strong argument and support for further,
366 more targeted research into Pediocin PA-1 and other bacteriocins. With colon cancer expected to
367 cause 52,980 deaths in the United States in 2021¹, and cervical cancer behind the cause of two
368 deaths a day in the UK⁴⁴, better treatment options need to be explored. With current conventional
369 chemotherapy treatments causing significant central and peripheral neurotoxic effects⁴, bacteriocins
370 such as those studied here offer the ability to target cancer cells whilst avoiding damage to other
371 healthy human cells. By understanding the mechanism by which Pediocin PA-1 works, we can either
372 isolate it for use in further studies and trials or derive a synthetic compound which works in a similar
373 way.

374

375

376

377

378

379

380

381

382

383

384

385

386

387

388

389

390

391

392

393

394

395

396

397

398 References

- 399 1. Cancer Research UK, <https://www.cancerresearchuk.org/health-professional/cancer->
400 [statistics-for-the-uk](https://www.cancerresearchuk.org/health-professional/cancer-statistics-for-the-uk) - heading-Zero Accessed: April 2021
- 401 2. Coudray, Anne-Marie; et al. "Proliferation of the Human Colon Carcinoma Cell Line HT29:
402 Autocrine Growth and Deregulated Expression of the c-myc Oncogene". *Cancer*
403 *Research*. 49: 6566–6571.
- 404 3. Scherer W.F., Syverton J.T., Gey G.O. Studies on the propagation in vitro of poliomyelitis
405 viruses. IV. Viral multiplication in a stable strain of human malignant epithelial cells (strain
406 HeLa) derived from an epidermoid carcinoma of the cervix. *J Exp Med*. 1953 May;97(5):695-
407 710.
- 408 4. Verstappen CC, Heimans JJ, Hoekman K, Postma TJ. Neurotoxic complications of
409 chemotherapy in patients with cancer: clinical signs and optimal management. *Drugs*.
410 2003;63(15):1549-63. doi: 10.2165/00003495-200363150-00003. PMID: 12887262.
- 411
- 412 5. Durand, T.; Bernier, M.; Léger, I.; Taillia, H.; Noël, G; Psimaras, D; *et al*. Cognitive outcome
413 after radiotherapy in brain tumor, *Current Opinion in Oncology*: 2015; Volume 27 - Issue 6 -
414 p 510-515
- 415
- 416 6. The Lancet. Breast cancer targeted therapy: successes and challenges. *The Lancet*. 2017.
417 Available at: [https://www.thelancet.com/journals/lancet/article/PIIS0140-6736\(17\)31662-](https://www.thelancet.com/journals/lancet/article/PIIS0140-6736(17)31662-8/fulltext)
418 [8/fulltext](https://www.thelancet.com/journals/lancet/article/PIIS0140-6736(17)31662-8/fulltext) – articleInformation Accessed April 2021
- 419
- 420 7. Camidge DR. Targeted therapy vs chemotherapy: which has had more impact on survival in
421 lung cancer? Does targeted therapy make patients live longer? Hard to prove, but impossible
422 to ignore. *Clin Adv Hematol Oncol*. 2014 Nov;12(11):763-6.
- 423

- 424 8. Cascales, E., Buchanan, S.K., Duche, D., Kleanthous, C., Llobes, R., Postle, K., Riley, M.,
425 Slatin, S., & Cavard, D.. Colicin biology. *Microbiology and molecular biology reviews* : MMBR.
426 2007. Vol.71, No.1, pp. 158-229, ISSN 1092-2172
427
- 428 9. Lwoff A., *Biochemistry and Physiology of Protozoa*. 1951. New York: Academic Press pp434
429
430
- 431 10. Kaur S., Kaur S. Bacteriocins as Potential Anticancer Agents. *Frontiers in Pharmacology*. 2015
432 6 pp 272
433
- 434 11. Villarante, K. I., Elegado, F. B., Iwatani, S., Zendo, T., Sonomoto, K., & de Guzman, E. E.
435 Purification, characterization and in vitro cytotoxicity of the bacteriocin from *Pediococcus*
436 *acidilactici* K2a2-3 against human colon adenocarcinoma (HT29) and human cervical
437 carcinoma (HeLa) cells. *World Journal of Microbiology and Biotechnology*. 2011. 27(4), 975–
438 980.
439
- 440 12. Bieler, S., Estrada, L., Lagos, R., Baeza, M., Castilla, J., & Soto, C. Amyloid formation
441 modulates the biological activity of a bacterial protein. *Journal of Biological*
442 *Chemistry*280(29), 26880–26885
443
- 444 13. Hetz, C., Bono, M. R., Barros, L. F., & Lagos, R. Microcin E492, a channel-forming bacteriocin
445 from *Klebsiella pneumoniae*, induces apoptosis in some human cell lines. *Proceedings of the*
446 *National Academy of Sciences of the United States of America*, 2002. 99(5), 2696–2701
447
- 447 14. Ankaiah D., Palanichamy E., Bharathi C., Ayyanna R., Perumal V., Basheer S. et al.

- 448 Cloning, overexpression, purification of bacteriocin enterocin-B and structural analysis,
449 interaction determination of enterocin-A, B against pathogenic bacteria and human cancer
450 cells. *International Journal of Biological Macromolecules*. 2018. 116 pp: 502-512
- 451 15. Bruno, M. E. C., & Montville, T. J. Common mechanistic action of bacteriocins from lactic acid
452 bacteria. *Applied and Environmental Microbiology*. 1993. 59(9), 3003–3010.
- 453 16. Bruno, M. E. C., & Montville, T. J. (1993). Common mechanistic action of bacteriocins from
454 lactic acid bacteria. *Applied and Environmental Microbiology*, 1993. 59(9), 3003–3010.
- 455 17. Abengózar MÁ, Cebrián R, Saugar JM, Gárate T, Valdivia E, Martínez-Bueno M, Maqueda M,
456 Rivas L. Enterocin AS-48 as Evidence for the Use of Bacteriocins as New Leishmanicidal
457 Agents. *Antimicrob Agents Chemother*. 2017 Mar 24;61(4):e02288-16.
- 458 18. Bayley, Jean-Pierre^a; Devilee, Peter^{a,b} The Warburg effect in 2012, *Current Opinion in*
459 *Oncology*. 2012. (1) 24
- 460 19. Gambhir, S. Molecular imaging of cancer with positron emission tomography. *Nat Rev*
461 *Cancer* 2, 683–693 (2002)
- 462 20. Annibaldi A, Widmann C. *Glucose metabolism in cancer cells*. *Curr Opin Clin Nutr Metab*
463 *Care* 2010;13(4):466-70
- 464 21. Espitia P., Otoni C.G., Soares N.F.F. Chapter 36 – Pediocin Applications in Antimicrobial Food
465 Packaging. *Antimicrobial Food Packaging*, Academic Press. 2016. Pp: 445-454
- 466 22. The UniProt Consortium
467 UniProt: the universal protein knowledgebase in 2021
468 *Nucleic Acids Res*. 2021. 49:D1
- 469 23. Waterhouse, A., Bertoni, M., Bienert, S., Studer, G., Tauriello, G., Gumienny, R., Heer, F.T., de
470 Beer, T.A.P., Rempfer, C., Bordoli, L., Lepore, R., Schwede, T. SWISS-MODEL: homology
471 modelling of protein structures and complexes. *Nucleic Acids Res*. 2018.v 46(W1), W296-
472 W303

- 473 24. Bienert, S., Waterhouse, A., de Beer, T.A.P., Tauriello, G., Studer, G., Bordoli, L., Schwede, T.
474 The SWISS-MODEL Repository - new features and functionality. *Nucleic Acids Res.* 2017. 45,
475 D313-D319
- 476 25. Guex, N., Peitsch, M.C., Schwede, T. Automated comparative protein structure modeling
477 with SWISS-MODEL and Swiss-PdbViewer: A historical perspective. *Electrophoresis* 2009. 30,
478 S162-S173.
- 479 26. Corpet F. Multiple sequence alignment with hierarchical clustering. *Nucl. Acids Res.* 1988.
480 16 (22), 10881-10890
- 481 27. Humphrey, W., Dalke, A. and Schulten, K., "VMD - Visual Molecular Dynamics", *J. Molec.*
482 *Graphics*, 1996, vol. 14, pp. 33-38
- 483 28. RCSB PDB, 2020. <https://www.rcsb.org/structure/3FXI> Accessed: April 2021
- 484 29. Bertoni, M., Kiefer, F., Biasini, M., Bordoli, L., Schwede, T. Modeling protein quaternary
485 structure of homo- and hetero-oligomers beyond binary interactions by homology. *Scientific*
486 *Reports* 7 (2017).
- 487 30. De Lorenzo, V. (1984). Isolation and characterization of nitrogenase from *Klebsiella*
488 *pneumoniae*. *Arch. Microbiol.*, 139, 72–75. [https://doi.org/10.1016/0076-6879\(86\)18097-9](https://doi.org/10.1016/0076-6879(86)18097-9)
- 489 31. De Lorenzo, V., & Pugsley, A. P. Microcin E492, a low-molecular-weight peptide antibiotic
490 which causes depolarization of the *Escherichia coli* cytoplasmic membrane. *Antimicrobial*
491 *Agents and Chemotherapy*. 1985. 27(4), 666–669.
- 492 32. Elmore, S. Apoptosis: A Review of Programmed Cell Death. *Toxicol. Pathol.* 2007. 35: 495.
- 493 33. RCSB PDB, 2020. <https://www.rcsb.org/> Accessed: April 2021
- 494 34. Fathizadeh, H., Saffari, M., Esmaeili, D., Moniri, R., Salimian, M. Evaluation of antibacterial
495 activity of enterocin A-colicin E1 fusion peptide. *Iranian Journal of Basic Medical Sciences*,
496 2020; 23(11): 1471-1479.

- 497 35. Pilchová, T., Pilet, M. F., Cappelier, J. M., Pazlarová, J., & Tresse, O. Protective effect of
498 *Carnobacterium* spp. against *Listeria monocytogenes* during host cell invasion using in vitro
499 HT29 model. *Frontiers in Cellular and Infection Microbiology*. 2016. 6(AUG)
- 500 36. Katare, P.B., Nizami, H.L., Paramesha, B. *et al.* Activation of toll like receptor 4 (TLR4)
501 promotes cardiomyocyte apoptosis through SIRT2 dependent p53 deacetylation. *Sci Rep*
502 2020. 10, 19232.
- 503 37. Katsnelson MA, Rucker LG, Russo HM, Dubyak GR. K⁺ efflux agonists induce NLRP3
504 inflammasome activation independently of Ca²⁺ signaling. *J Immunol*. 2015 Apr
505 15;194(8):3937-52
- 506 38. Kennedy CL, Smith DJ, Lyras D, Chakravorty A, Rood JI. Programmed cellular necrosis
507 mediated by the pore-forming alpha-toxin from *Clostridium septicum*. *PLoS Pathog*.
508 2009;5(7):e1000516
- 509 39. Jiang X, Yuan J, Dou Y, Zeng D, Xiao S. Lipopolysaccharide Affects the Proliferation and
510 Glucose Metabolism of Cervical Cancer Cells Through the FRA1/MDM2/p53 Pathway. *Int J*
511 *Med Sci* 2021; 18(4):
512
- 513 40. Furrie, E., Macfarlane, S., Thomson, G., Macfarlane, G.T. *et al.*, Toll-like receptors-2, -3 and -4
514 expression patterns on human colon and their regulation by mucosal-associated bacteria.
515 *Immunology* 2005; 115: 565-574
- 516 41. Takeuchi O, Hoshino K, Kawai T, Sanjo H, Takada H, Ogawa T, Takeda K, Akira S. Differential
517 roles of TLR2 and TLR4 in recognition of gram-negative and gram-positive bacterial cell wall
518 components. *Immunity*. 1999 Oct;11(4):443-51
- 519 42. Chen Y, Shapira R, Eisenstein M, Montville TJ. Functional characterization of pediocin PA-1
520 binding to liposomes in the absence of a protein receptor and its relationship to a predicted
521 tertiary structure. *Appl Environ Microbiol*. 1997 Feb;63(2):524-31. doi:
522 10.1128/AEM.63.2.524-531.1997. PMID: 9023932; PMCID: PMC168344.

523 43. Moll GN, Konings WN, Driessen AJ. Bacteriocins: mechanism of membrane insertion and
524 pore formation. *Antonie Van Leeuwenhoek*. 1999 Jul-Nov;76(1-4):185-98.

525 44. Cancer Research UK, <https://www.cancerresearchuk.org/health-professional/cancer->
526 [statistics/statistics-by-cancer-type/ovarian-cancer](https://www.cancerresearchuk.org/health-professional/cancer-statistics/statistics-by-cancer-type/ovarian-cancer) Accessed: April 2021

527

528

529

530

531

532

533

534

535

536

537

538

539

540

541

542

543

544

545

546

547

548

549 Appendix

550 **S2 Fig. 2 Sequence Alignment of Microcin E492 and Pediocin PA-1**

551 **S2 Fig. 3 VMD 3D model of Pediocin and Microcin Interacting with TLR-4**

552 **S2 Fig. 4 VMD 3D Model of Pediocin PA-1 Interacting with TLR-4**

553 **S2 Fig. 5 MultiAlign Sequence Alignment of Pediocin PA-1 and Enterocin heterodimer A and B**

554 **S2 Fig. 6 VMD 3D Model of Enterocin A**

555 **S2 Fig. 7 SWISSMODEL 3D Model of Enterocin B**

556 **S2 Fig. 8 MultiAlign Sequence Comparison of Divercin V41 and Pediocin PA-1**

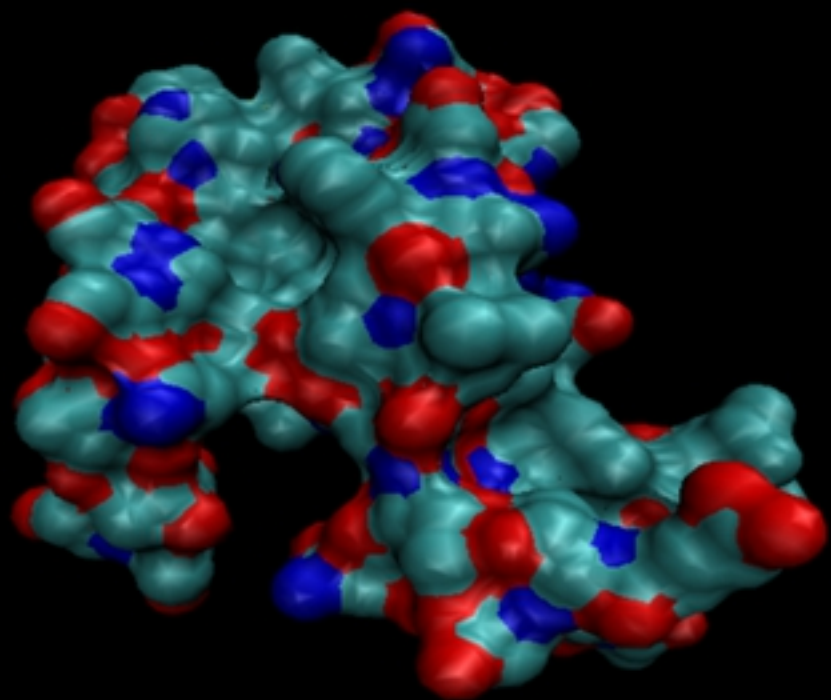
557 **S2 Fig. 9 SWISSMODEL 3D Devised Model of Divercin V41 and Pediocin PA-1**

558

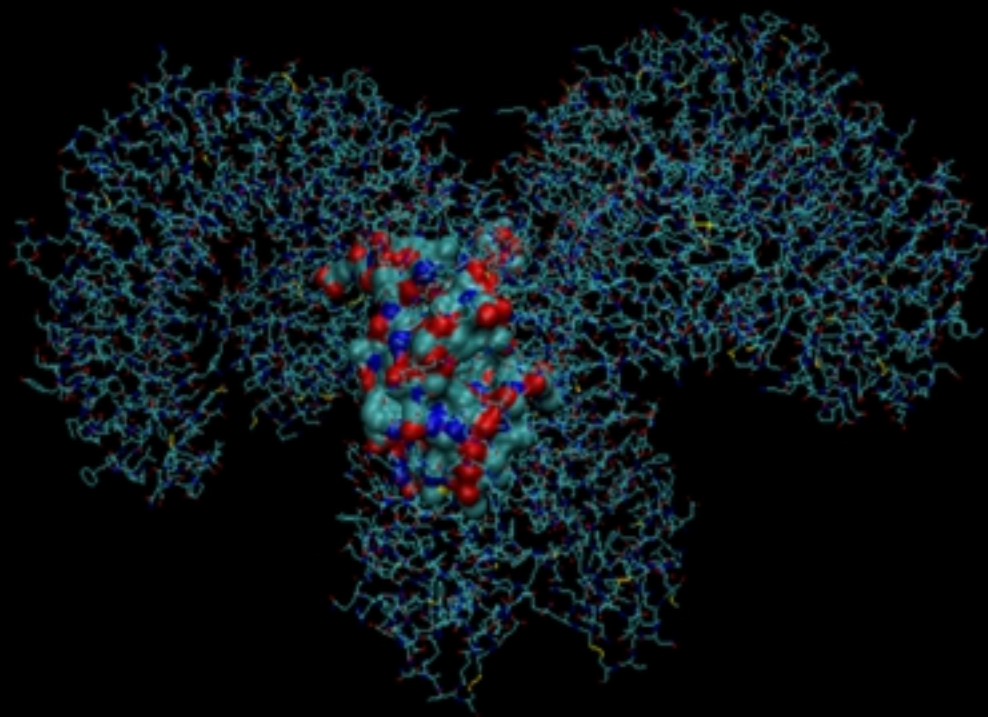
559



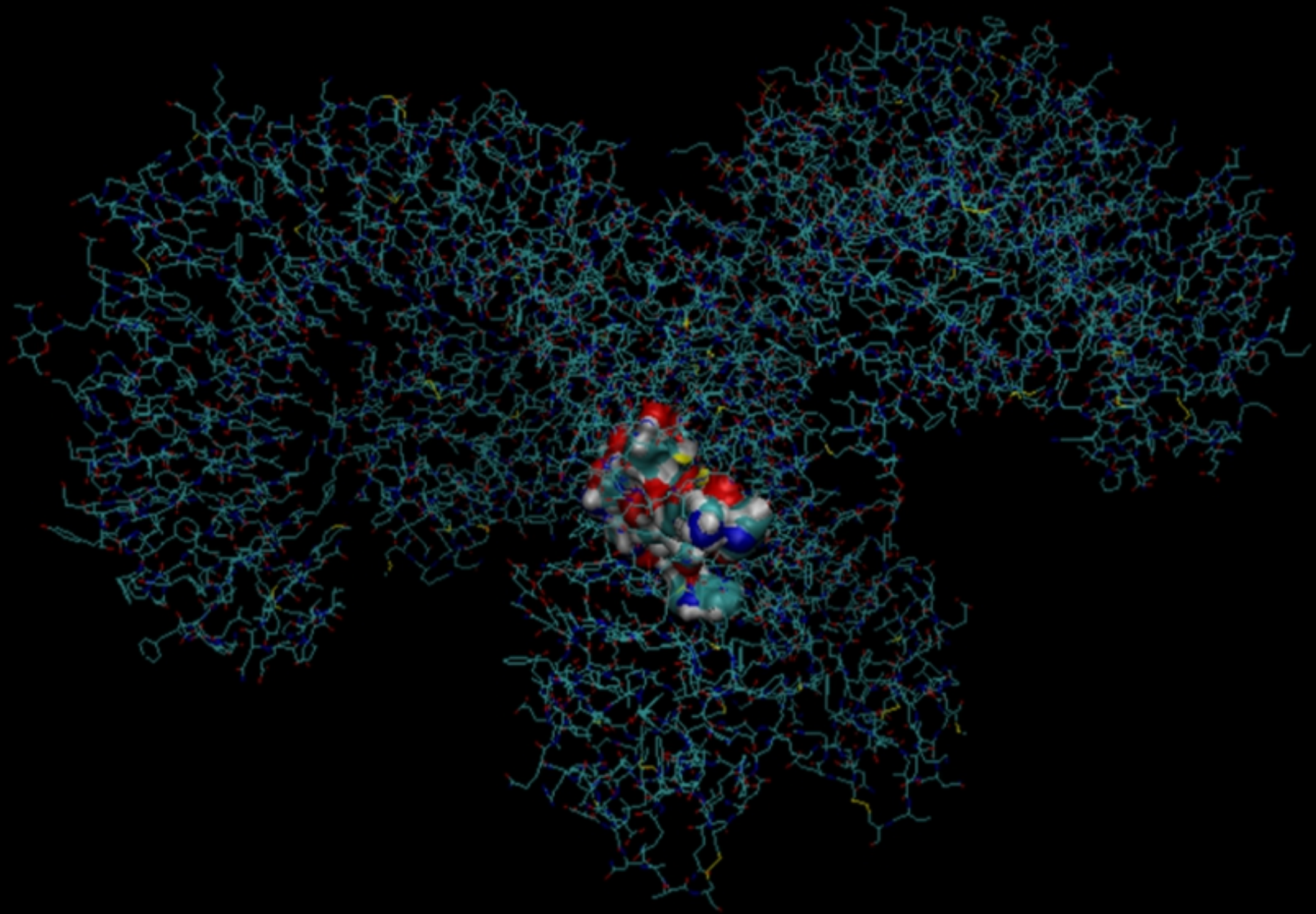
S2 Fig2



A)



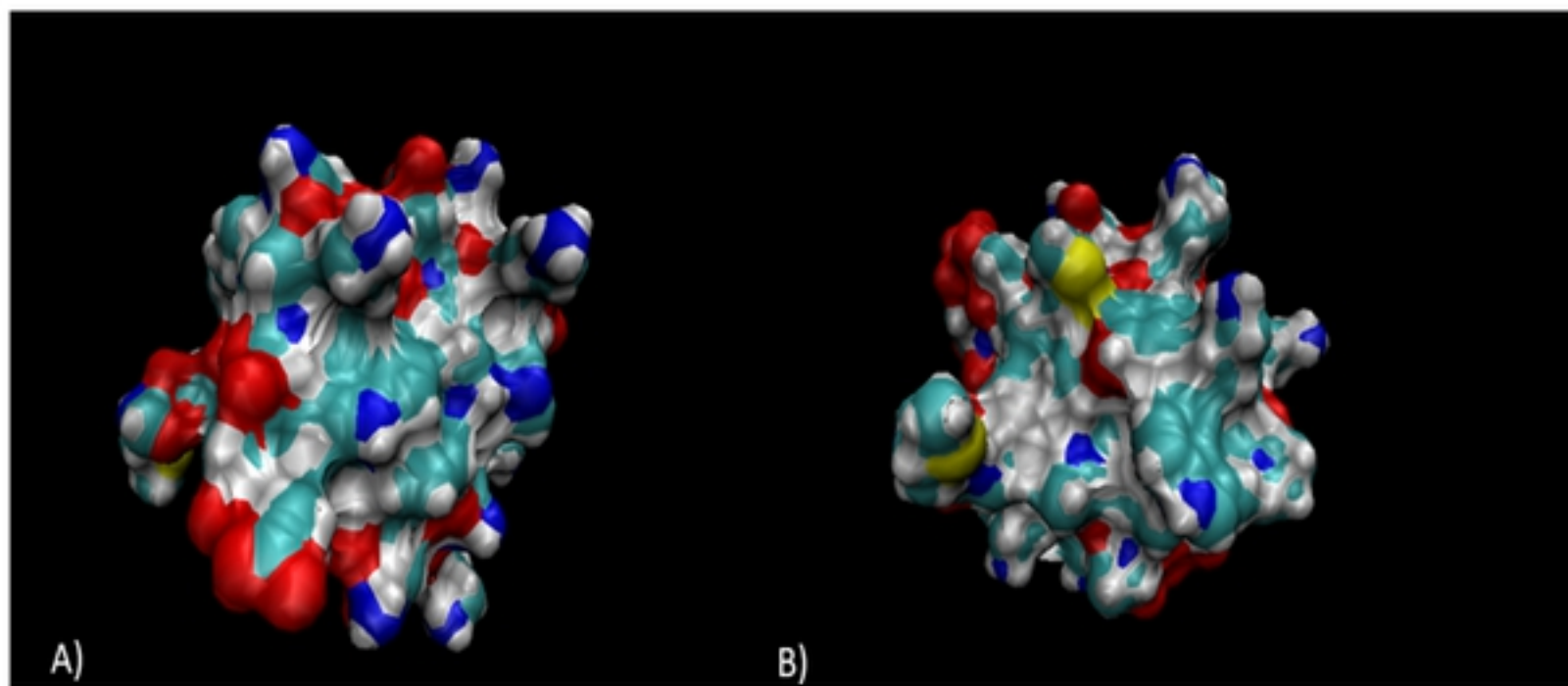
B)



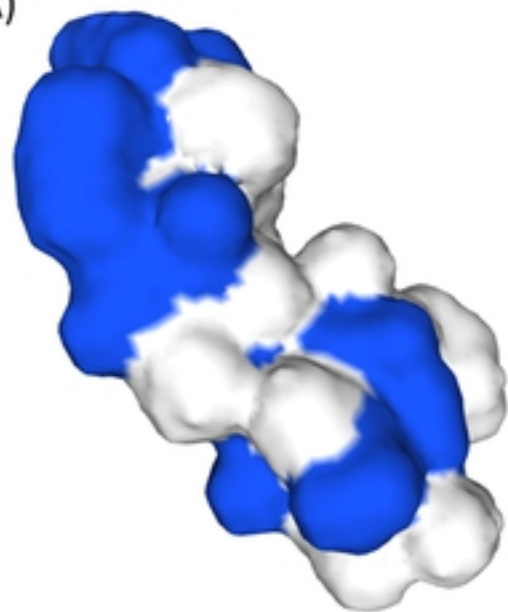
S2 Fig4

	1	10	20	30	40	50	60	70	72																																																														
	-----+	-----+	-----+	-----+	-----+	-----+	-----+	-----+																																																															
sp P29430 Pediocin	M	K	I	E	K	L	T	E	K	E	M	A	N	I	I	G	G	-	-	-	-	K	-	-	-	-	Y	Y	G	N	G	V	T	C	G	K	H	S	C	S	Y	D	W	G	K	A	T	T	C	I	I	N	N	G	A	M	A	W	A	T	G	G	H	Q	G	N	H	K	C		
tr Q9L658 EntA	M	K	H	L	K	I	L	S	I	K	Q	T	Q	L	I	Y	G	G	T	T	H	S	G	K	-	-	-	-	Y	Y	G	N	G	V	Y	C	T	K	N	K	C	T	Y	D	W	A	K	A	T	T	C	I	A	G	M	S	I	G	G	F	L	G	G	A	I	P	G	-	-	K	C
tr O34017 EntB	M	Q	N	Y	K	E	L	S	T	K	E	M	K	Q	I	I	G	G	E	N	D	H	R	M	P	N	E	L	N	R	P	N	N	L	S	K	G	G	A	K	C	G	A	I	A	G	G	L	F	G	I	P	-	K	G	P	L	A	W	A	A	G	L	A	N	Y	Y	S	K	C	N
Consensus	M	k	.	k	.	L	s	.	K	#	n	.	I	i	G	G	k	y	y	G	N	g	v	.	c	g	k	.	k	C	.	v	d	w	a	k	a	t	t	c	I	.	.	g	.	.	a	w	a	.	G	.	.	.	g	.	.	K	C	.		

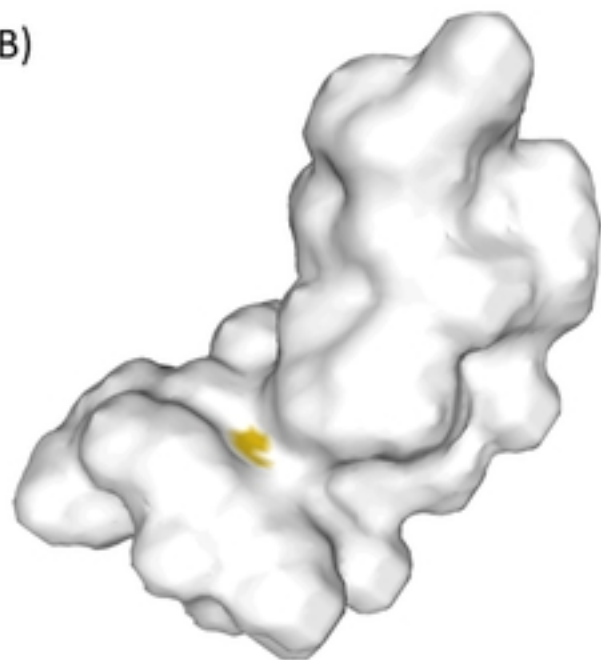
S2 Fig5



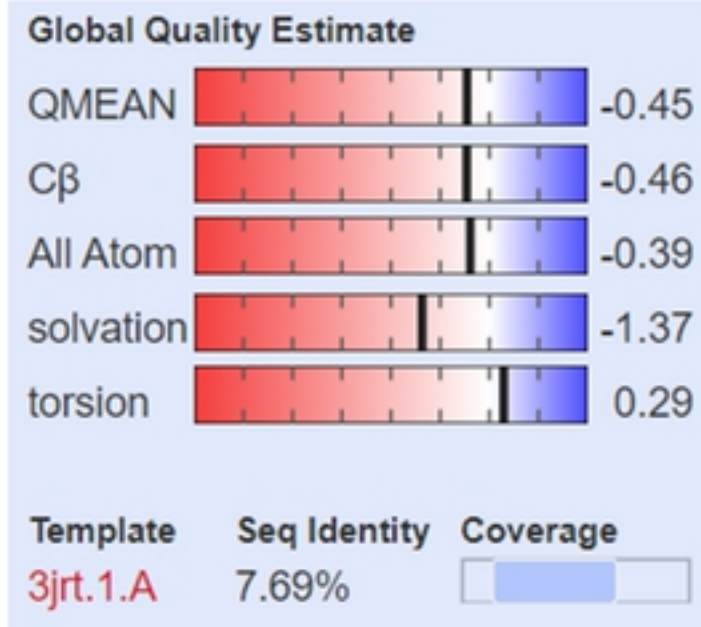
A)

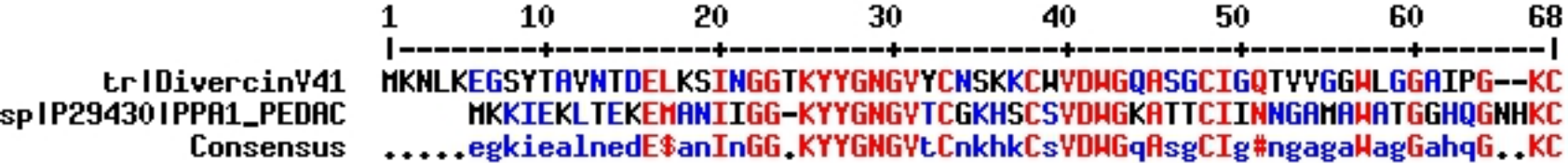


B)

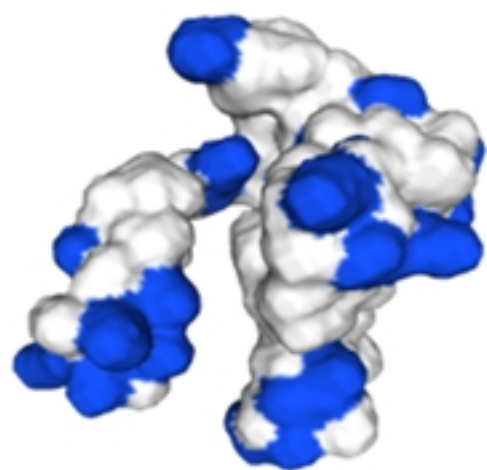


C)

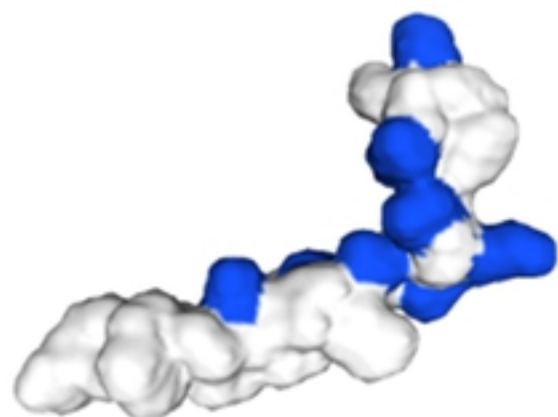
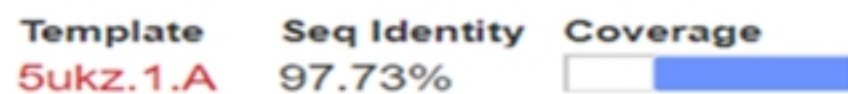
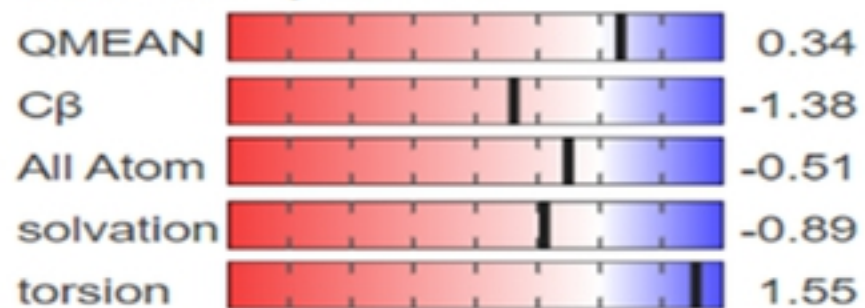




S2 Fig8



Global Quality Estimate



Global Quality Estimate

